Stem Cell Reports
Article

ISSCR

OPEN ACCESS

Notch activation during early mesoderm induction modulates emergence of the T/NK cell lineage from human iPSCs

Dar Heinze,[1,3] Seonmi Park,[1] Andrew McCracken,[1] Mona Haratianfar,[1] Jonathan Lindstrom,[1] Carlos Villacorta-Martin,[1] Aditya Mithal,[1] Feiya Wang,[1] Meng Wei Yang,[1] George Murphy,[1] and Gustavo Mostoslavsky[1,2,*]

[1]Center for Regenerative Medicine of Boston University and Boston Medical Center, Boston, MA, USA
[2]Department of Medicine, Section of Gastroenterology at Boston University and Boston Medical Center, Boston, MA, USA
[3]Department of Surgery, Boston University Medical Center, Boston, MA, USA
*Correspondence: gmostosl@bu.edu
https://doi.org/10.1016/j.stemcr.2022.10.007

SUMMARY

A robust method of producing mature T cells from iPSCs is needed to realize their therapeutic potential. NOTCH1 is known to be required for the production of hematopoietic progenitor cells with T cell potential *in vivo*. Here we identify a critical window during mesodermal differentiation when Notch activation robustly improves access to definitive hematopoietic progenitors with T/NK cell lineage potential. Low-density progenitors on either OP9-hDLL4 feeder cells or hDLL4-coated plates favored T cell maturation into TCRab$^+$CD3$^+$CD8$^+$ cells that express expected T cell markers, upregulate activation markers, and proliferate in response to T cell stimulus. Single-cell RNAseq shows Notch activation yields a 6-fold increase in multi-potent hematopoietic progenitors that follow a developmental trajectory toward T cells with clear similarity to post-natal human thymocytes. We conclude that early mesodermal Notch activation during hematopoietic differentiation is a missing stimulus with broad implications for producing hematopoietic progenitors with definitive characteristics.

INTRODUCTION

Induced pluripotent stem cells (iPSCs) are an ideal starting source for differentiating T cells for therapeutic purposes. They offer a tractable platform for precise and confirmed introduction of germline modifications including chimeric antigen receptors, safety features (e.g., inducible death genes), and reducing immunogenicity. These modifications can be pre-validated, making them potentially safer than alternative methods of T cell production. Potential clinical applications include oncology, autoimmunity, or even tolerance induction in transplantation depending on the subset of T cells in question. For these reasons, a robust method of T cell differentiation from iPSCs is of great clinical interest.

Successful differentiation of iPSC-derived T cells is dependent on the robust generation of T-capable progenitors. During embryogenesis, hematopoietic development begins with primitive hematopoiesis, a transient wave of limited erythro-myeloid progenitors and culminates with definitive hematopoiesis and the production of the true hematopoietic stem cell (HSC). Primitive and definitive hematopoiesis are both spatially and temporally separated, with primitive cells arising in the extra-embryonic mesoderm (such as the yolk sac) and definitive cells arising from the endothelium of the aorta and other major vessels through an endothelial to hematopoietic transition. In mice and zebrafish, T cell potential arises after the primitive wave but before the true HSC. These initial T-capable progenitors develop from the aortic endothelium although some arise from a more mature yolk sac population (Boiers et al., 2013; Tian et al., 2017; Yoshimoto et al., 2012). Thus the developmental origin of HSCs and some of the earliest T-capable progenitors is shared with arterial endothelium. The development of arterial endothelium involves the medial migration and arterial specification of the lateral plate mesoderm, a process dependent on many signaling pathways including Notch, WNT, SHH, and VEGF (Fish and Wythe, 2015).

In particular, the Notch pathway is critical for arterial specification and the formation of HSCs (Clements et al., 2011; Hadland et al., 2004; Kumano et al., 2003). The Notch pathway consists of four receptors (NOTCH1–4) and delta/jagged ligands. Notch receptors are activated by the mechanical force of ligand endocytosis, which exposes the receptor to cleavage by gamma-secretase to release the Notch intracellular domain, which drives Notch-dependent gene expression in the nucleus (Gordon et al., 2015). *In vitro* studies have demonstrated the importance of the Notch pathway in hematopoiesis (Ditadi et al., 2015; Leung et al., 2018). These studies used small molecule inhibitors of the Notch pathway to show it was required for differentiating progenitors with increased lineage capacity. In another study, the Notch pathway was activated using a plate-bound dll4-Fc fusion protein at day 4 of differentiation. This led to the formation of an "arterial" phenotype to the resulting hemogenic endothelial cells (CD144$^+$, CD73$^-$) that went on to produce progenitors with improved T potential (Uenishi et al., 2018). Montel-Hagen and colleagues created a three-dimensional (3D)

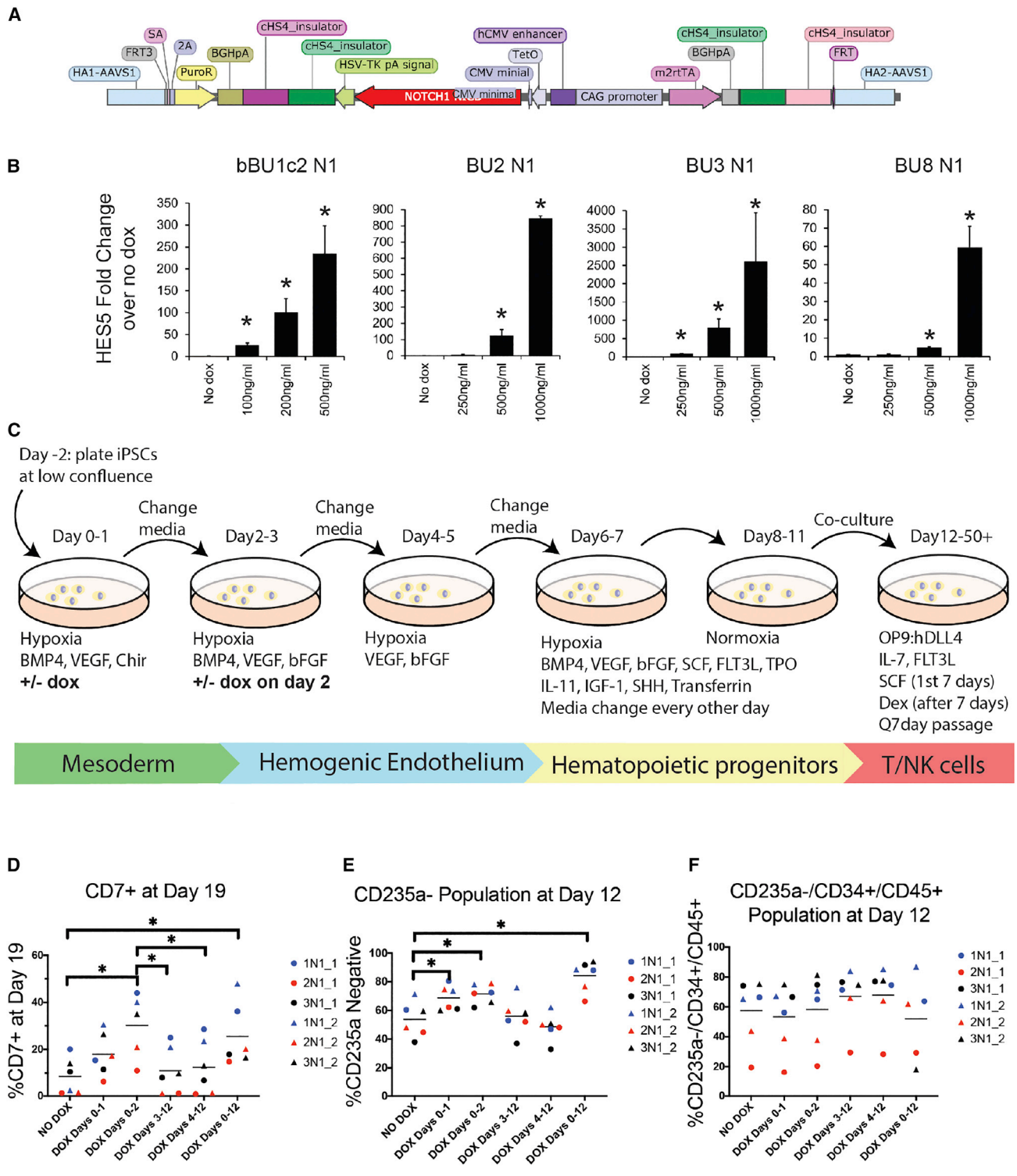

Figure 1. Notch activation during mesoderm induction robustly specifies the emergence of iPSC-derived hematopoietic progenitors with T cell competence

(A) Diagram showing the TetOn:NICD1 construct for AAVS1 targeting. The cHS4 insulators reduce silencing and the T2A:puro is used for selection. The m2rtTA is included under the control of a separate CAG promoter.

(legend continued on next page)

artificial thymic organoid by aggregating a putative human embryonic mesodermal progenitor ($CD326^{-}CD56^{+}$) from day 3 of differentiation with a mouse bone marrow stromal cell line expressing human DLL4 (MS5-DLL4). These differentiating cells went on to produce CD8SP T cells (Montel-Hagen et al., 2019). Thus inhibiting Notch reduces lineage potential while stimulating it increases lineage potential of the resulting hematopoietic progenitors.

However, none of these studies pursued the timing or intensity of Notch activation needed to facilitate the emergence of T-capable progenitors. In this study, we sought to address these questions by developing iPSC lines with an inducible promoter driving the expression of the intracellular domain of the NOTCH1 receptor (NICD1). This approach allows autonomous control over the Notch pathway, as it does not rely on the expression of NOTCH1 or Notch ligands. Using an optimized 12 day hematopoietic progenitor differentiation protocol, we identified the first 72 h of differentiation as a critical time period when activation of the Notch pathway increased T/natural killer (NK) cell commitment up to 10-fold by day 19 as measured by live $hCD7^{+}$ cells. These cells could be influenced toward T or NK cell fates on the basis of the density of progenitors introduced into the system, with lower density favoring T cell differentiation.

T cells matured through a DP ($CD4^{+}CD8^{+}$) stage to a $CD7^{+}CD3^{+}CD8^{+}CD4^{-}$ cell consistent with CD8SP cells. Our protocol favors robust emergence of $TCRab^{+}CD8ab^{+}$ cells. These cells could be activated by CD3/CD28 tetramers to express activation markers and proliferate. Finally, we undertook single-cell sequencing of our T cell cultures at very early stages as well as from the progenitor stage (day 12) to late DP stage (day 42) compared with post-natal human thymocytes. This revealed that early Notch activation yielded a population of multi-potent day 12 progenitors that was 6-fold larger than untreated cells. Macrophage, erythrocyte, and NK cell fates were accessed by our progenitors, but the majority of cells progressed toward T cells with a gene expression signature similar to that of post-natal human thymocytes. We conclude that early Notch stimulation promotes the development of multi-potent hematopoietic progenitors with robust NK and T cell potential that mature into functional CD8SP cells.

RESULTS

Notch activation during mesoderm induction robustly specifies the emergence of iPSC-derived hematopoietic progenitors with T cell competence

To control the activation of the Notch pathway, we developed four iPSC lines with a TetOn promoter driving the expression of the intracellular domain of the NOTCH1 receptor inserted into the AAVS1 locus (Figure 1A). Positive clones showed a dose-responsive increase in expression of the Notch target gene *HES5* in response to doxycycline (dox) treatment (Figure 1B). We then used an optimized 12 day two-dimensional (2D) hematopoietic progenitor differentiation protocol, based on our work and that of others (Ditadi and Sturgeon, 2016; Leung et al., 2018; Takata et al., 2017) (the "iT protocol"; Figure 1C) to discover the timing and intensity of Notch activation needed to maximize T/NK-capable progenitor production. Using human CD7 expression as an indicator of T/NK lineage output after 1 week of co-culture with OP9 cells expressing hDLL4, we discovered that Notch activation during the first 72 h of differentiation (days 0–2) was critical for specifying progenitors with T cell lineage potential (Figure 1D). In an effort to uncover surface markers expressed on day 12 progenitors that predict T/NK capacity, we plotted populations negative for CD235a (Figure 1E) or $CD235a^{-}/CD34^{+}/CD45^{+}$ (Figure 1F) across the same conditions of doxycycline treatment. These results show that the best indicator of future T/NK competence at day 12 was the percentage of CD235a-negative cells as opposed to the percentage of $CD34^{+}$ cells. Using a combination of KDR (VEGFR2), CD34, and VE cadherin as markers of putative hemogenic endothelium, we confirmed that cells that are high KDR^{+} indeed identified cells at day 4 capable of giving rise to $CD235a^{-}CD34^{+}CD45^{+}$ hematopoietic progenitors (Figure S1).

(B) Dose-response curve for Notch target gene HES5 after doxycycline (0–1,000 ng/mL) treatment for 72 h for each of the 4 Tet-On:NICD1 lines made. Three biological replicates (separate wells with independent RNA extractions) of each condition were used, error bars are SD, data shown are fold change calculated by delta-deltaCt method with BACT as control gene, $*p < 0.05$ from two-tailed t test compared with untreated control.

(C) Schematic of the iT differentiation protocol outlining cytokines, media changes, and timing of each intervention. The putative developmental stage of the differentiation is shown underneath, from mesoderm to T/NK cells.

(D) Early T/NK cells measured by $\%CD7^{+}$ population using flow cytometry at day 19 (after one week of co-culture on OP9:hDLL4 feeder cells) for untreated, dox-treated from days 0–1, 0–2, 3–12, 4–12, and 0–12. Horizontal bars mark the average of each sample. Statistical significance assessed using 2-tailed t test with $p < 0.05$. N = 6 separate differentiations (2 differentiations for 3 different TetOn:NICD1 lines: bBU1c2:N1 [1N1], BU2:N1 [2N1], and BU3:N1 [3N1]).

(E and F) These show the same experiment as in (D), except they show the CD235 negative ($CD235a^{-}$) population and the $CD235a^{-}/CD34^{+}/CD45^{+}$ population (respectively) at day 12 from each of the doxycycline treatment conditions.

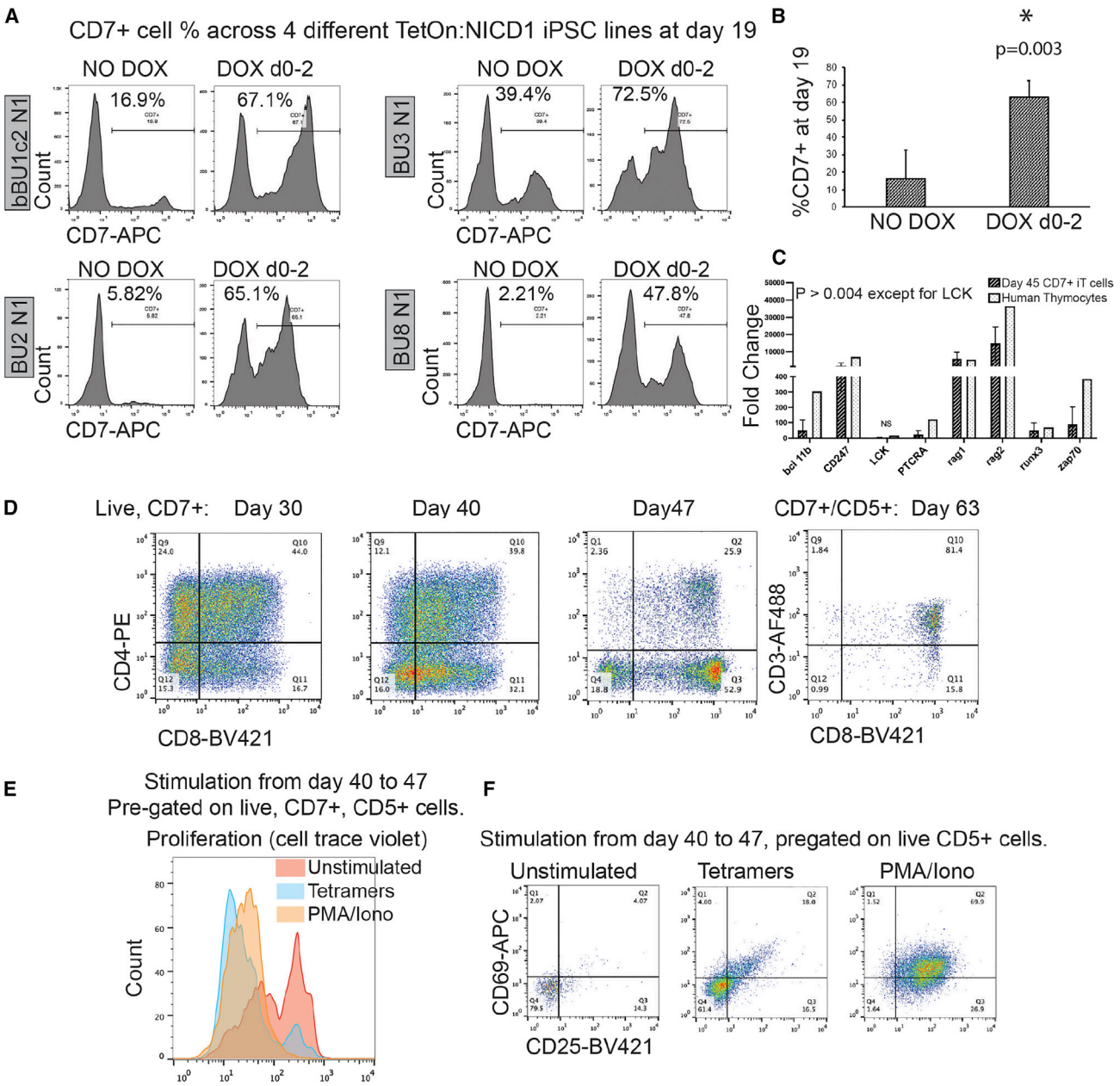

Figure 2. CD7$^+$ cells generated from the iT protocol mature into T cells

(A) All 4 TetOn:NICD1 lines were differentiated to day 19 with and without doxycycline treatment from days 0 to 2 (doxycycline concentrations were 100 ng/mL for 1N1, 350 ng/mL for 3N1, and 500 ng/mL for 2N1 and 8N1). This experiment shows that the increase in CD7$^+$ cells at day 19 in dox-treated cultures is consistent across 4 independent iPSC lines.

(B) The %CD7 cells at day 19 as observed in (A) was averaged (±SD) for the treated and untreated samples and the difference was statistically significant with $p < 0.003$ using a 2-tailed t test.

(C) Gene expression of a panel of T cell-related transcripts in day 45 CD7$^+$ FACS-sorted cells and human thymocytes compared with iPSCs. Four separate differentiations were sorted at day 45 (N = 2 for 2 separate cell lines [1N1, 3N1]). Fold change was calculated by the delta-deltaCt method with BACT as control gene. Significance was assessed using t test compared with iPSCs ($p < 0.004$ except for LCK, which was not significant). Error bars are SD.

(D) Representative flow cytometry evaluating expression of CD4, CD8, and CD3 from day 30 to day 63 of differentiation for 1N1. N > 5 separate differentiations to day 47. N = 2 separate differentiations for day 63.

(legend continued on next page)

We differentiated all 4 TetOn:NICD1 iPSC lines with and without day 0–2 doxycycline treatment and analyzed the percentage of $CD7^+$ cells at day 19 (Figures 2A and 2B). Early Notch stimulation induced robust and reproducible emergence of T/NK-capable progenitors across all 4 iPSC lines. Following incubation of day 19 $CD7^+$ cells in conditions favoring T cell specification (see experimental procedures and Table S1), we analyzed differentiated cells at day 45 for the expression of characteristic T cell genes by quantitative real-time PCR. As shown in Figure 2C, day 45 $CD7^+$ iPSC-derived T cells express *RAG1*, *RAG2*, *ZAP70*, *LCK*, and *BCL11B* (among others) at similar levels to freshly isolated post-natal human thymocytes (Figure 2C). Using flow cytometry, we followed T cell maturation from day 30 to day 63 and observed appropriate developmental progression with early emergence of CD4 immature single-positive (CD4ISP) cells, followed by $CD4^+/CD8^+$ DP cells, and finishing with the production of $CD7^+/CD5^+/CD3^+/CD8^+$ cells (Figure 2D). Stimulation of day 40 iPSC-derived T cells using either CD3/CD28 tetramers or PMA/ionomycin induced robust proliferation (Figure 2E) and upregulation of activation markers CD25 and CD69 (Figure 2F). The tetramers were less efficient than PMA/ionomycin, likely because of the fact that at day 40, expression of CD3 was not robust yet.

Notch activation is required for T/NK lineage competence in a time-dependent manner

In order to further define the mechanism behind our findings, we sought to identify the cell population activating the Notch pathway early in our differentiations by using fluorescence-activated cell sorting (FACS). We isolated three populations at day 3: KDR^- (putative non-mesodermal population), $KDR^+CD34^-VECadherin^-$ (putative mesoderm), and $KDR^+CD34^+VECadherin^+$ (putative hemogenic endothelium) and compared the expression of Notch genes between these populations in both dox-treated and untreated cultures (Figure 3A). In the untreated state, no significant upregulation of Notch genes was noted between the KDR^+ and KDR^- populations (data not shown). In contrast, significant upregulation of *NOTCH1*, *NOTCH4*, *HEY1*, *DLL4*, and *JAG2* was observed between the KDR^- and $KDR^+/CD34^+/VECadherin^+$ populations that was more pronounced in the Notch-induced sample (Figure 3A). Notch is known to cause both cell-cycle arrest and progression in different systems (Joshi et al., 2009; Noseda et al., 2004), an effect that could have an impact on the timing of fate determination between dox-treated and untreated differentiations. To address this possibility, we measured the percentage of cells in G1 and G2 at day 3 of differentiation and found no difference between no-dox and plus-dox conditions (Figure 3B), strongly suggesting the effect of early Notch induction in hematopoietic lineage specification is not influenced by changes in cell-cycle status.

To further define the dynamics of early hematopoietic specification, we tracked the percentage of KDR^+ and $KDR^+CD34^+VECadherin^+$ populations from day 2 to day 6 of differentiation using flow cytometry (Figures S2A and S2B). Notch induction led to a small but significant increase in the KDR^+ population, but did not significantly change the percentage of $KDR^+/CD34^+/VECadherin^+$ cells. In addition, the percentage of floating $CD235a^-/CD34^+/CD45^+$ hematopoietic progenitors was tracked from days 8–12 between dox-treated and untreated cultures, and no significant difference was observed (Figure S2C). Overall, these data demonstrate that doxycycline-driven Notch activation in our system does not lead to significant cell cycle changes or modify the timing or percentage of hematopoietic progenitors produced on the basis of this limited set of surface markers.

Using DAPT (a gamma-secretase inhibitor that blocks Notch signaling) and our TetOn:NICD1 system, we verified that the Notch pathway is required for the production of progenitors with T potential and that doxycycline can partially rescue this phenotype (Figure S2D). In an effort to understand the kinetics of Notch pathway activation during differentiation, we followed the expression of Notch target genes *HEY1* and *HES5* as well as *KDR* as a marker of mesodermal specification during the first 8 days of the iT protocol (Figure 3C). We analyzed these data comparing each day with day 1 of the parental differentiation (day 2 with day 1, day 3 with day 1, etc.) in both dox-treated tet-on:NICD1 lines as well as dox-treated parental lines. Notably, during the differentiation of all 4 parental (not targeted) lines, we observed a significant induction of Notch signaling starting at day 4 of differentiation. In contrast, in all 4 dox-inducible iPSC lines, addition of doxycycline stimulated a much earlier and robust induction of Notch signaling, as evidenced by a 50-fold increase in *HES5* and a 12-fold increase in *HEY1* expression at day 2 of differentiation. These data provide strong evidence supporting that in our iT protocol, Notch signaling is normally induced at day 4 of differentiation. However, by forcing induction of Notch signaling immediately after addition of doxycycline into the culture we developed an early window of accessibility that drives the emergence of more definitive hematopoiesis and eventually translates into

(E and F) Day 40 cells were stimulated for 7 days with CD3/CD28 tetramers or PMA/ionomycin (25 ng/mL and 250 ng/mL, respectively) in the presence of 5 ng/mL IL-2 and activation assessed using Cell Trace Violet to monitor proliferation (pre-gated on live, $CD7^+/CD5^+$ cells, see E) and surface markers of activation CD69 and CD25 (pre-gated on live $CD5^+$ cells, see F). 1N1 line, N = 2 separate differentiations.

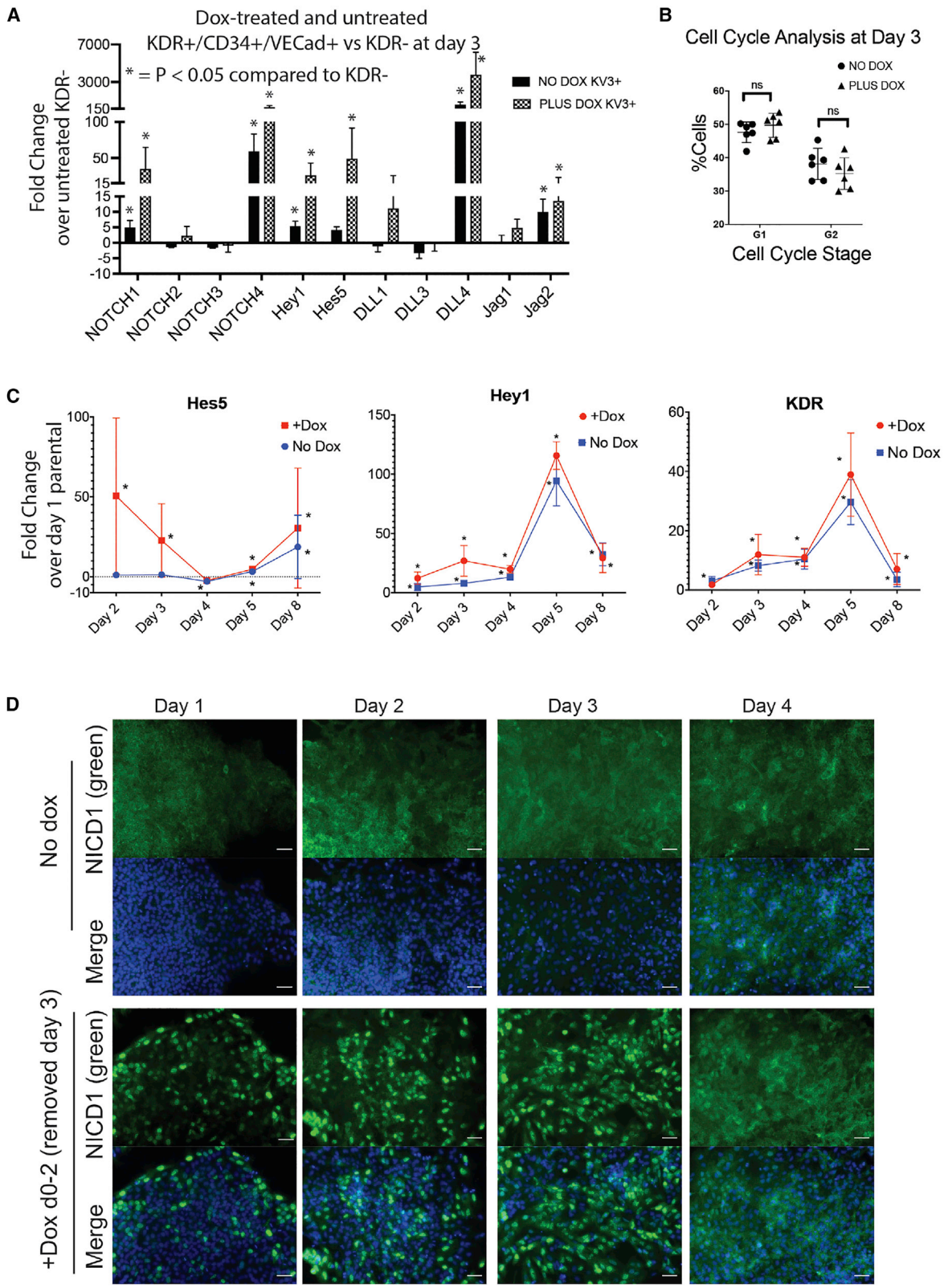

(legend on next page)

the production of progenitors with T/NK potential. In addition, these data also explain why doxycycline treatment after day 2 had no effect in the differentiation protocol (i.e., the Notch pathway is already on). In agreement with our previous data showing an increase in KDR expression as measured using flow cytometry, we detected a significant increase in KDR gene expression following doxycycline treatment and Notch induction (Figure 3C). In order to confirm NICD1 expression at the protein level, we monitored NICD1 across the first 4 days of the iT protocol by immunofluorescence, comparing no dox versus dox treatment. As shown in Figure 3D, bright nuclear NICD1 staining was already evident by day 1 of dox treatment and was sustained during all 3 days of dox induction, rapidly diminishing by day 4 when doxycycline was already removed from the culture. Overall, our results provide strong evidence that the Notch pathway is normally activated early during the emergence of the hemogenic endothelial cell population in our iT protocol. Using our TetOn:NICD1 system we induced an earlier and stronger Notch activation that did not influence cell cycle progression or the percentage of progenitors expressing CD34 but still yielded a robust increase in progenitors with T/NK lineage potential.

Hematopoietic progenitors produced in the iT protocol have both T and NK cell potential

In several of our differentiations, we observed a striking phenotype between day 19 and 40 showing the rapid loss of the OP9 stromal layer (Figure 4A). Characterization of the differentiated cells using flow cytometry showed they lost the T cell marker CD5 and upregulated expression of the NK cell marker CD56. In order to define the factors that determine the T versus NK cell lineage decision, we tested several culture variables in high-density cultures (>250,000 day 12 progenitors/10 cm plate) including modulating serum concentration, IL-7 concentration, and Notch activation (both inhibiting with DAPT and activating it with dox) and found that none of these altered NK lineage specification (data not shown). Strikingly, changing the plating density of day 12 progenitors transferred on top of the OP9 feeder layer was found to dramatically impact the outcome, with low density (50,000–100,000/10 cm plate) favoring T cell differentiation and higher density (>100,000/10 cm plate) favoring emergence of NK cells (Figure 4B). Indeed, the loss of $CD5^+$ cells nicely correlated with the increase in density and the appearance of $CD56^+$ cells. These $CD56^+$ cells expressed other NK markers such as NKp44, NKG2D, and NKp46 (Figure 4C).

Notch drives an accelerated induction of nascent mesoderm

To investigate the events underlying the increase in T cell potential following notch activation, single-cell RNA (scRNA) sequencing was performed on iPSCs on days 2, 3, and 4 of differentiation (Figure S3). This demonstrated progression through the primitive streak and nascent mesoderm at day 2, mesoderm by day 3, and endothelial progenitors at day 4 (Figures S3A and S3B). In addition, small populations of contaminating ectodermal and endodermal cells were noted. The effect of notch activation induced prominent differences in clustering at day 2 between doxycycline and DMSO-treated cultures (Figure S3C). The induction of notch at day 2 could be demonstrated by the upregulation of notch target genes such as HES4 (Figure S3D). Using gene lists identified by Tyser et al. (2021) from scRNA sequencing of gastrulating human embryos (see Table S2), notch induction promoted an earlier shift from primitive streak to nascent mesodermal fates (Figures S3E and S3F). These data strongly suggest that earlier induction of mesodermal fate underlies the

Figure 3. Notch activation is required for T/NK lineage competence in a time-dependent manner

(A) Notch genes are expressed in the putative hemogenic endothelial population at day 3. Day 3 dox-treated and untreated cultures were FACS-sorted into KDR^- (non-mesoderm) and $KDR^+CD34^+VECadherin^+$ (putative hemogenic endothelium) populations for 1N1, 2N1, and 3N1. Real-time PCR showed significant expression of a broad range of notch genes (*NOTCH1*, *NOTCH4*, *HEY1*, *HES5*, *DLL4*, and *JAG2*) only in the putative hemogenic endothelial population. However, upregulation of notch target genes was increased in all populations in the dox-treated cells compared with the untreated (data not shown). Significance assessed at $p < 0.05$ using 2-tailed t test from KDR^- population, and error bars are SD (N = 3 separate differentiations).

(B) Cell cycle analysis of dox-treated and untreated cultures at day 3. G1 and G2 populations were assessed using flow cytometry of ethanol-fixed, DAPI-stained samples. The percentage of cells in each phase was recorded and significance assessed using t test. Horizontal bars represent the mean ± SD (N = 6 separate differentiations, 2 each for 1N1, 2N1, and 3N1).

(C) Gene expression analysis of notch targets *HES5*, *HEY1*, and mesodermal marker *KDR* comparing all 4 TetOn:NICD1 lines and their parental (non-targeted lines) treated with doxycycline (100 ng/mL for bBU1c2:N1 [1N1] and 250 ng/mL for the others [2N1, 3N1, 8N1]). Non-targeted parental lines were treated with doxycycline to control for any doxycycline effect outside of the inducible promoter. Samples were collected from days 1 to 8 of differentiation. Each sample was compared with day 1 of the parental differentiation and significance assessed using t test with $p < 0.05$ considered significant. Average fold change ± SD is shown.

(D) Representative staining for NICD1 (AF488 green) and nuclei (Hoescht blue) in BU2-TetOn:NICD1 (2N1) in dox-treated (days 0–2) and untreated differentiations on days 1–4. Data are representative of 3 separate differentiations (1N1, 2N1, 3N1). Images shown taken with 20× objective; scale bars, 30 μM.

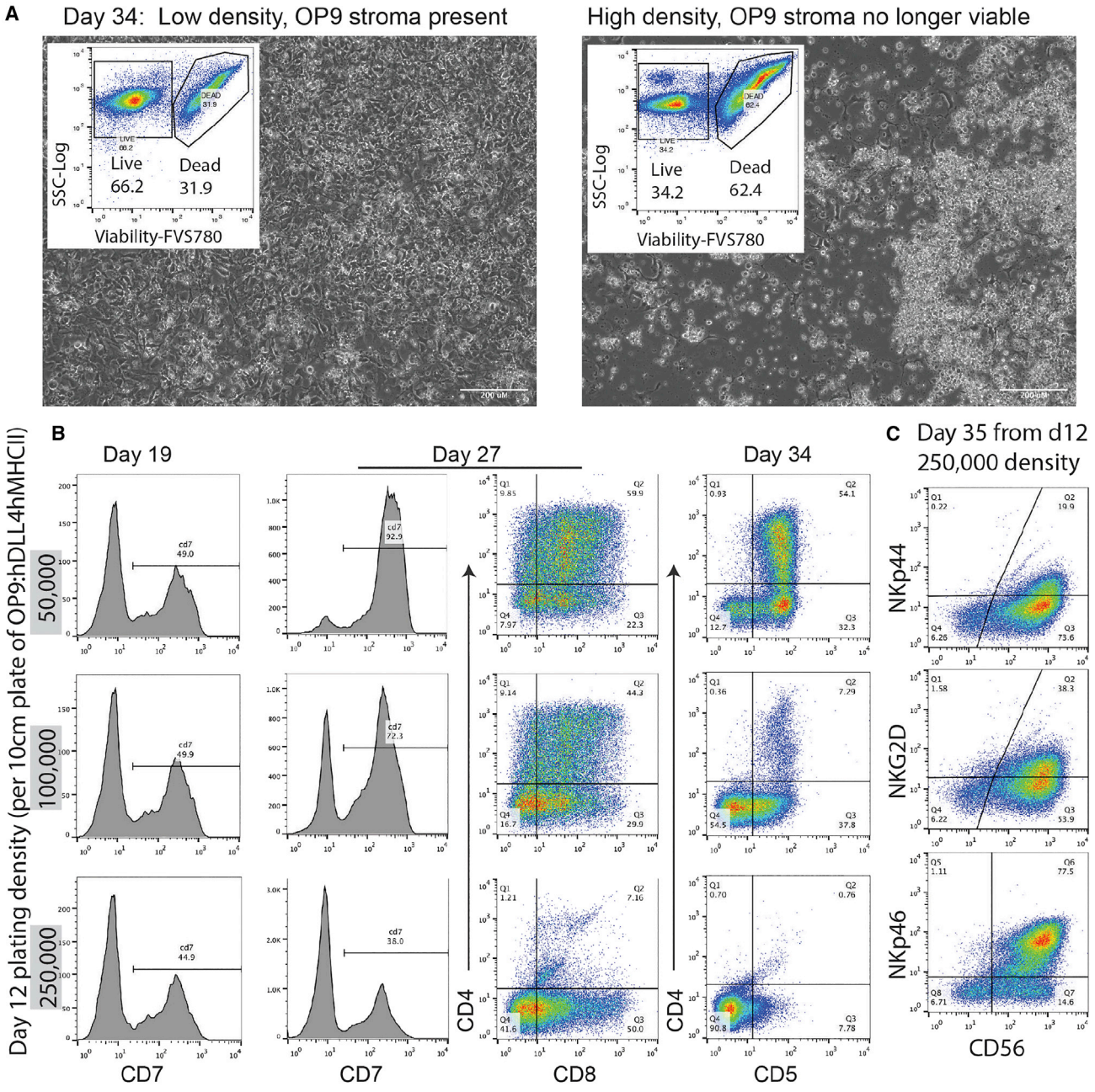

Figure 4. Hematopoietic progenitors produced in the iT protocol have both T and NK cell potential

(A) Day 34 10× objective bright-field images of low (left) and high (right) density cultures showing loss of OP9 stroma and increase in debris (scale bar, 200 μM). Inset: staining for live versus dead cells shows the significant increase in the percentage of dead cells under high density conditions. N = 5 separate differentiations with 1N1.

(B) Representative flow cytometry from days 19–34 in cultures with 3 different densities (50,000 progenitors/10 cm plate of OP9:hDLL4 at day 12, 100,000, and 250,000). Day 19 shows CD7% only. Day 27 shows $CD7^+$ population and $CD4^+/CD8^+$ population. Day 34 shows $CD4^+/CD5^+$ population. A marked loss of $CD7^+$ and $CD4^+/CD5^+$ double-positive cells is shown as the progenitor density increases. N = 4 separate differentiations with 1N1, representative flow cytometry shown.

(C) Flow cytometry showing percentage of NK cells expressing CD56 and NKp44, NKG2D, or NKp46 at day 35 of differentiation in the co-culture plated with 250,000 cells at day 12. For this staining, N = 2 separate differentiations with 1N1.

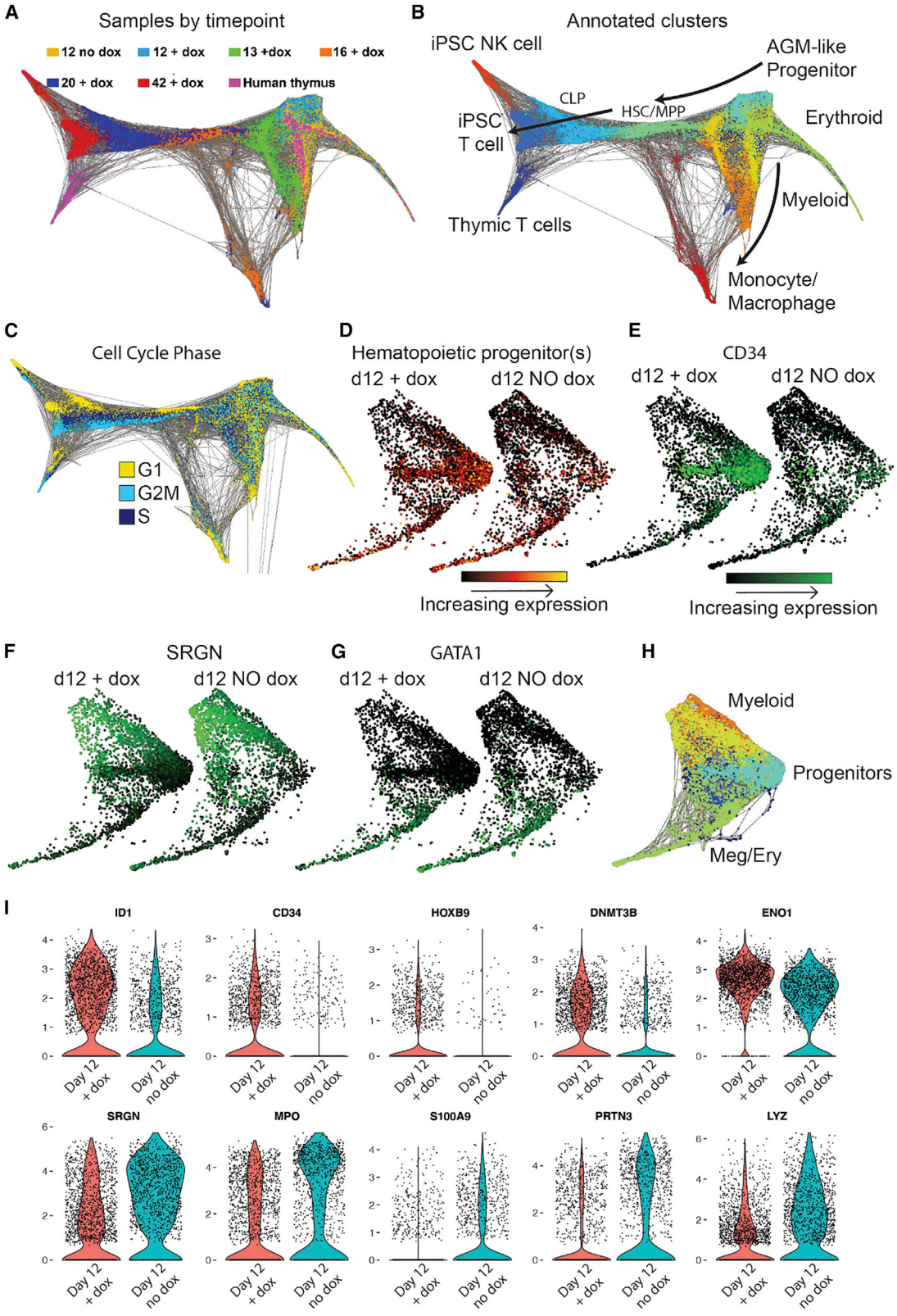

(legend on next page)

enhanced definitive hematopoietic differentiation evidenced in our protocol upon notch induction.

Single-cell RNA sequencing supports a developmental trajectory from progenitors to T cells

To better characterize the effect of Notch activation on our day 12 progenitor cells and to follow the developmental program of these progenitors as they develop into early T cells, we pursued single-cell RNA sequencing at 5 time points from days 12 to 42 compared with freshly isolated post-natal human thymocytes (Figure S4A). We also included a comparison of day 12 progenitors from dox-treated (days 0–2) and untreated cultures, to determine the global transcriptional impact of early Notch induction on these day 12 progenitors. We chose time points to capture the transition to the co-culture environment (day 13), the initiating events toward the T/NK lineage (day 16), the emergence of T/NK lineage cells (day 20), and the late double-positive ($CD4^+CD8^+$) T cells (day 42). These time points were selected on the basis of our flow cytometry data (see Figures 1D and 2D). We ran biological duplicates (two separate differentiations) of all samples except the human thymus with a capture of 1,400–2,200 cells per sample. In all, we sequenced 22,832 cells with a read depth of 41,000 reads/cell and a weighted average of unique molecular identifier (UMI) counts/cell of 4,133. Louvain clustering of all 7 samples was visualized in SPRING (Figure 5A), yielding 12 clusters at a resolution of 0.25 in the full dataset (Figure 5B). Analysis of cell cycle showed differences in cell cycle phase throughout the entire dataset (Figure 5C), but these differences did not drive Louvain clustering at any time point (Figures 5B and 5C). We then ran Gene Ontology analysis using EnrichR (Chen et al., 2013; Kuleshov et al., 2016) on each cluster combined with previously reported lineage-specific gene lists identified using single-cell sequencing of human fetal liver (Popescu et al., 2019) and additional gene lists that we generated on the basis of a literature search (Table S3). When we put these data together, the spring plot showed a clear developmental trajectory from progenitors containing erythroid and myeloid cells progressing to at least two defined clusters separating the monocyte/macrophage lineage from the lymphoid lineage resolving into a defined T/NK signature (Figure 5B).

Early Notch activation induces a robust increase in multi-potent progenitors

In order to specifically define the effect of early Notch induction on the day 12 progenitor population, we generated a spring plot focusing on the dox-treated and untreated day 12 samples (Figure 5D). Although the hematopoietic progenitor gene list clearly identified cells in both dox-treated and untreated samples, early Notch induction has a major impact on the number and distribution of canonical progenitors at day 12 (Figure 5D). The dox-treated samples contributed 87% of the cells in this cluster (1,959), while the untreated progenitors contributed only 13% (327). A spring plot highlighting CD34 expression shows a high degree of overlap with this cluster, supporting its progenitor identity (Figure 5E). Putative myeloid clusters collectively express characteristic genes such as *SRGN* (Figure 5F). The dox-treated and untreated cultures contribute 40% (998) and 60% (1,453) of the total cells in these clusters. A final cluster expresses early erythroid/megakaryocyte genes such as *GATA1* (Figure 5G) with a contribution of 44% (670) and 56% (867) of cells from dox-treated and untreated progenitors. Overall, this analysis defined the presence of a progenitor population that is clearly enriched in the Notch-induced sample, and putative myeloid and Meg/Ery cells over-represented in the untreated sample (Figure 5H). In a head-to-head comparison, the top 5 upregulated genes in the day 12 dox-treated progenitors were strongly associated with hematopoietic stem/progenitor

Figure 5. Single-cell RNA sequencing supports a developmental trajectory from progenitors to T cells

Single-cell RNA sequencing of developing T cells from day 12 progenitors to day 42 T cells (bBU1c2 and 1N1 iPSC line) and human thymocytes (primary cell control).

(A) All 22,832 cells from 7 separate samples was visualized in Spring. Each sample was color-coded by identity (day 12 no dox, day 12 + dox, day 13, day 16, day 20, day 42, and human thymus).

(B) The same full Spring plot shown in (A) now showing the Louvain clustering at 0.25 resolution with annotations of putative cell populations.

(C) Full Spring plot showing cell cycle phase for this experiment. Although some segregation by phase is noted after day 13, this did not influence the Louvain clustering seen in (B).

(D–G) Day 12 treated and untreated progenitors were separated from the rest of the analysis and visualized in Spring. The dox-treated and untreated cells were manually separated from each other by a constant amount so the differences in expression of genes could be appreciated; +dox cells on the left and no-dox cells on the right. The composite expression signature of a list of hematopoietic progenitor genes (Table S3) is shown in (D). Expression of the classic hematopoietic progenitor gene CD34 (E), a myeloid-related gene Serglycin (SRGN) (F), a Meg/erythroid gene GATA1 (G), with increased expression shown in green.

(H) Full Spring plot of day 12 progenitors showing main clusters annotated for progenitor, myeloid, and Meg/Ery groups.

(I) Violin plots showing top 5 most enriched up- and downregulated genes between dox-treated (red) and untreated (blue) day 12 progenitors.

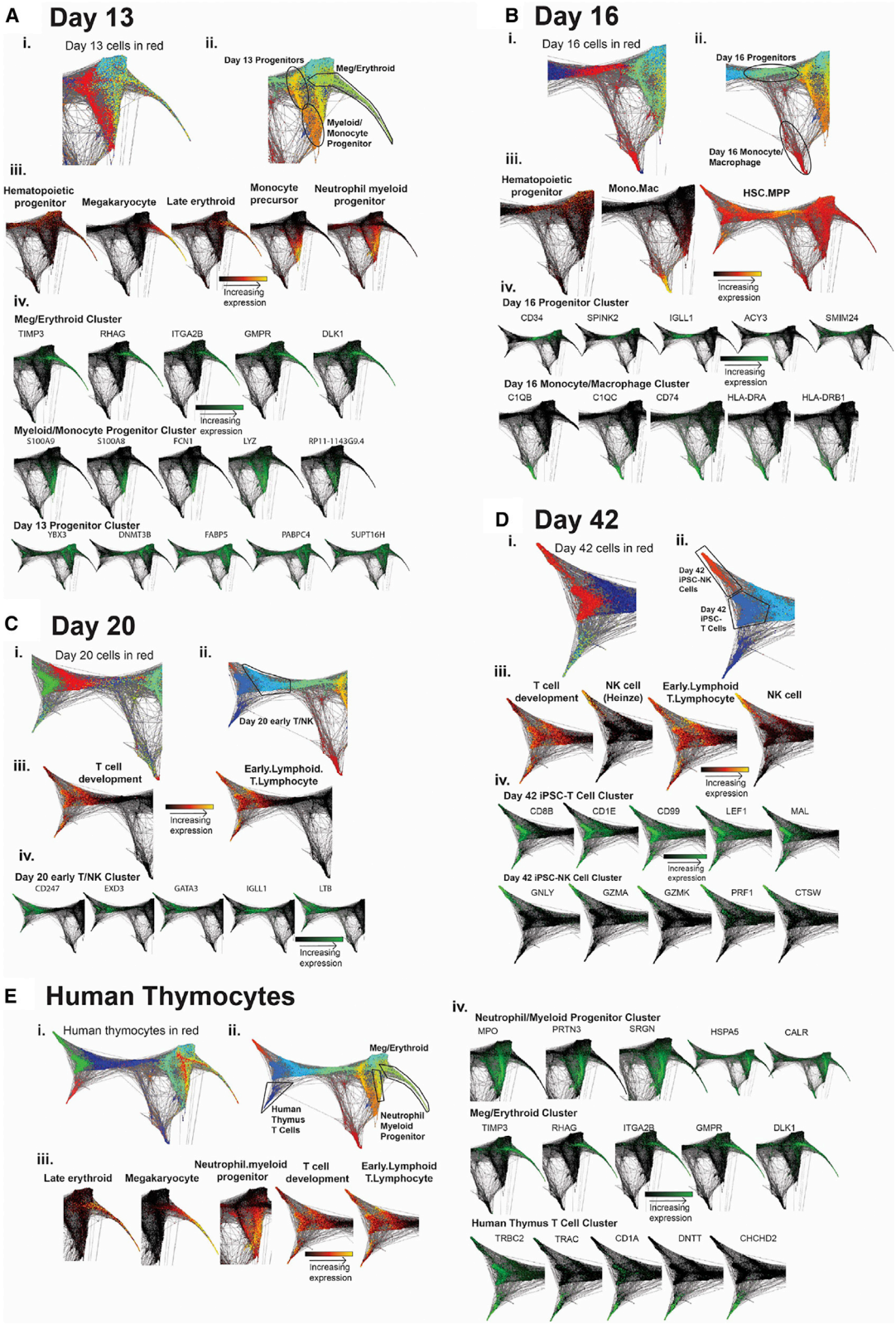

(legend on next page)

cells (HSPCs) (Figure 5I). These included *CD34*, the most common surface marker used to enrich HSPCs, *ID1* and *DNMT3B*, known to be involved in proliferating HSPCs poised for differentiation (Challen et al., 2014; Singh et al., 2018), and *HOXB9*, a gene that co-operates with other HOX-cluster genes to maintain HSPCs (Bijl et al., 2006; Lawrence et al., 2005). In contrast, genes downregulated supported a strong myeloid signature including serglycin (Niemann et al., 2007), myeloperoxidase (Paul et al., 2015), lysozyme (Kitaguchi et al., 2009), S100A9 (Roth et al., 2003), and proteinase 3 (Campanelli et al., 1990). In summary, our day 12 progenitors showed a cluster of cells expressing a gene signature consistent with multi-potent hematopoietic stem/progenitor cells that was 6-fold larger in the dox-treated than untreated cells. Both treated and untreated progenitors contributed cells to myeloid progenitor and erythroid/megakaryocyte progenitor clusters, with a higher proportion in the untreated cells. Overall, these data support a key role for early Notch activation driving the emergence of the HSPC population during differentiation.

Developmental trajectory toward T cells

Day 13 cells were analyzed to capture the early transcriptional events occurring after the change from the progenitor culture conditions to the co-culture environment (Figure 6Ai). In total, 3,468 cells were captured. These cells divide into 3 main clusters on the full spring plot (Figure 6Aii). Visualization of gene expression (on the basis of gene lists defined in Table S3) confirmed the presence of hematopoietic progenitors, meg/erythroid progenitor, and myeloid/monocyte progenitor cells (Figure 6Aiii). The day 13 progenitor cluster still expresses *DNMT3B* in the top 5 enriched genes (as in the day 12 progenitors) but showed expression of several genes active in transcription such as *YBX3* (putative repressor of the granulocyte-macrophage colony-stimulating factor [GM-CSF] promotor), *PABPC4* (binds to mRNAs to increase stability in activated T cells), and *SUPT16H* (interacts with histones to aid transcriptional elongation) (Figure 6Aiv). Gene Ontology provided only general terms, such as "$CD34^+$" (Human Gene Atlas) and "human embryo" (ARCHS4 Tissues) (Table S4). These results identify this cluster as transcriptionally active undifferentiated hematopoietic progenitors. As shown in Figure 6Aiv, the myeloid/monocyte progenitor cluster expressed myeloid genes such as lysozyme (*LYZ*) and the S100 family of calcium binding proteins (Roth et al., 2003). Gene Ontology analysis of this cluster shows a non-specific myeloid signature with myeloid, monocyte, dendritic cell and neutrophil-related terms (Table S4). Finally, a small population of day 13 cells (302 cells) remained in the Meg/erythroid cluster described in the day 12 sample.

We analyzed 3,667 cells from day 16 to assess an intermediate time point between day 13 and day 20 (when flow cytometry data shows a large population of $CD7^+$ cells) (Figure 6Bi). These cells divide into two main clusters in the full spring plot (Figure 6Bii). Gene expression signatures shown in Figure 6Biii indicate the identity of the day 16 clusters as hematopoietic progenitors and monocyte/macrophages. The day 16 progenitor cluster contains 2,016 cells that express progenitor genes such as *CD34*, *SPINK2*, and *SMIM24* but also lymphoid-associated genes such as *IGLL1* (part of pre-B cell receptor [Miyazaki et al., 1999]; Figure 6Biv). This is consistent with the co-expression of CD34 and early T cell markers in the thymus (Terstappen et al., 1992). However, it is interesting to note that 3 of the top 5 genes expressed in the day 16 progenitor cluster are also in the top 5 genes in the HSC.MPP gene list defined by single-cell sequencing of the human fetal liver (Popescu et al., 2019). This suggests an alternative interpretation that our day 12 progenitors represent an earlier hematopoietic progenitor that has now matured closer to the *in vivo* fetal liver HSC/MPP. This possibility is supported by Gene Ontology terms that for day 12 and 13 progenitors were not specific (human embryo, midbrain, human cortex, and kidney, human embryo, for days 12 and 13 respectively; see Table S4) but for day 16 Gene Ontology analysis is able to identify specifically hematopoietic progenitors: $CD34^+$ (Human Gene Atlas), $CD34^+$ cell, bone marrow (bulk tissue), and cord blood (ARCHS4 Tissues) (Table S4). The day 16 monocyte/macrophage cluster contained 965 cells. This cluster showed CD74, complement, and MHC II components as the top 5 enriched genes (Figure 6Biv). Gene Ontology analysis and visualization of a monocyte/macrophage gene list support the identity of these cells as monocyte/macrophages. In addition, Gene

Figure 6. Developmental trajectory toward T cells

(A–E) Day 13 (A), day 16 (B), day 20 (C), day 42 (D), and human thymocytes (E) are shown. For each time point, the cells are shown in red to highlight their location in the full spring plot (i). The Louvain clusters identified by the cells in each sample are annotated in (ii). In (iii), the gene expression signatures of lineage-specific gene lists are shown, with low expression in black and highest expression in yellow (see Table S3 for gene lists; note that "(Heinze)" refers to gene list[s] compiled from the literature by the first author of this paper). The top 5 enriched genes in each cluster annotated for that sample are shown in (iv). For these plots, low expression is black and higher expression is shown in green. This pattern is repeated for (A)–(E). Although all clustering is shown from the full dataset, the individual images are cropped to conserve space when possible (i.e., expression data not lost).

Ontology analysis highlighted antigen processing and presentation of peptide antigens (GO: 0002478) as significant terms suggesting the presence of antigen-presenting cells in our co-cultures (Table S4). We conclude that the progenitor cluster identified at days 12 and 13 matures toward a progenitor that more closely resembles human fetal liver HSCs by day 16. However, these progenitors also express lymphoid-related genes, suggesting early commitment toward the lymphoid lineage at this time point. The myeloid progenitor cluster observed at days 12 and 13 was not prominent at day 16 but was instead replaced by a cluster of putative monocyte/macrophages, suggesting maturation of the myeloid lineages by day 16.

On day 20, one major cluster was seen containing 2,827 of 3,677 cells (Figures 6Ci and 6Cii). A small number of cells remained in the progenitor and monocyte/macrophage clusters observed at day 16. The T cell development gene list and the early lymphoid T lymphocyte gene list from (Popescu et al., 2019) (Table S1) showed high concordance in identifying the main day 20 cluster as early lymphoid cells (Figure 6Ciii). Gene Ontology analysis provided more T cell-related terms such as Human Gene Atlas: leukemialymphoblastic(MOLT-4), thymus, CD8$^+$Tcells, and ARCHS4 Tissues: regulatory T cells, thymus, TLymphocyte (Table S4). The top 5 genes expressed in the day 20 early T/NK cluster include T cell-related genes *CD247* (CD3z) and *GATA3* as well as *LTB* (lymphotoxin beta) and *IGLL1*, earlier lymphoid genes (as in day 16). Overall, this analysis defines a population of early lymphoid cells maturing toward the T cell lineage (Figure 6Civ).

We analyzed 3,811 cells at day 42, representing a developmental time frame consistent with a late double-positive (CD4$^+$CD8$^+$) stage on flow cytometry (Figure 2D). At this time point, two clusters were present, a day 42 iPSC-T cell cluster containing 2,928 cells and a day 42 iPSC-NK cell cluster with 810 cells (Figures 6Di and 6Dii). These clusters were identified using a T cell and NK cell gene list derived from a literature search and the T lymphocyte and NK cell gene list from Popescu et al. (2019) (Figure 6Diii; Table S3). Gene Ontology supports these labels with the top terms for Human Gene Atlas and ARCHS4 Tissues being thymus, TLymphocyte, and CD4$^+$_Tcells for the T cell cluster and CD56$^+$_NKCells, TLymphocyte, and natural killer cells for the NK cell cluster (Table S4). The top 5 genes expressed in the T cell cluster include *CD1E*, *CD8B*, *MAL* (MyD88-adapter-like, involved in T cell signal transduction), and *LEF1* (TCF1/7, a transcription factor that binds to TCR alpha enhancer) (Figure 6Div). These data provide strong evidence for the presence of CD8$^+$ T cells as well as progression to a classic CD8ab T cell (as evidenced by expression of *CD8B*) and not abnormal CD8aa lymphocytes as previously reported (Themeli et al., 2013). The top transcripts in the NK cell cluster are granule components granulysin, cathepsin, and granzymes (Figure 6Div). This suggests that by day 42, our cultures contain a mixed population of ~75% T cells and ~25% NK cells.

To compare our iPSC-derived T cells with the closest human corollary, we sequenced 1,500 freshly isolated postnatal human thymocytes. On full spring clustering, two main groups are noted; the first is thymic T cells, which cluster very close to our day 42 iPSC-derived T cells, and the second group overlaps with the day 12 and 13 samples (Figures 6Ei and 6Eii). The latter group overlapped with two clusters already described earlier, the myeloid population from day 12 and the Meg/erythroid population seen at days 12 and 13 (Figures 5G and 6A). The thymic T cell cluster expresses *TRBC2* and *TRAC* (constant regions of the TCR beta and alpha chains), *CD1a*, and *DNTT* (a DNA polymerase that adds nucleotides at the junctions of the TCR gene segments) within the top 5 enriched genes (Figure 6Eiii). This suggests an immature alpha-beta T cell phenotype consistent with their thymic origin. During normal T cell development, TCR beta re-arrangement occurs before TCR alpha (Shah and Zuniga-Pflucker, 2014). Comparing our day 42 T cells and the human thymic T cells, both populations robustly express *TCRB2* (TCR beta constant region 2). However, in contrast to the thymic T cells, which most express *TRAC*, our iPSC-derived T cells showed few cells expressing *TRAC*, suggesting that our cells are just beginning to transition to TCR alpha expression at day 42 (Figure 6Eiv).

Here we have presented single-cell RNA sequencing data of 7 different samples defining the transcriptional signatures of iPSC-derived hematopoietic progenitors differentiating into T/NK cells. Notch activation during mesodermal differentiation yielded a robust enrichment of multipotent progenitor cells at day 12, and these cells showed a time-dependent progression toward the T cell lineage (evidenced by the loss of early hematopoietic genes and the appearance of specific lymphoid transcripts) that eventually mature into putative T cells expressing T cell markers such as *BCL11B*, *LEF1*, and *CD3D* (Figure S4B).

Feeder-free conditions support the emergence of alpha-beta T cells

In order to explore the differentiation potential of our iT protocol-derived cells using feeder-free conditions, we adapted the protocol to replace the use of OP9 feeders with coated plates optimized for the differentiation of T lymphocytes (see experimental procedures). As shown in Figure 7A, by day 40 the vast majority of the cells were CD5$^+$/CD7$^+$ cells, with a small proportion of CD7^{high}CD5^{low} cells expressing CD56. Approximately 35% of the CD5$^+$/CD7$^+$ population were also CD3$^+$. The CD3$^-$ cells expressed CD4 and CD8a consistent with an immature double-positive CD4/CD8 phenotype. Furthermore, up to 60% of the CD3$^+$ cells were

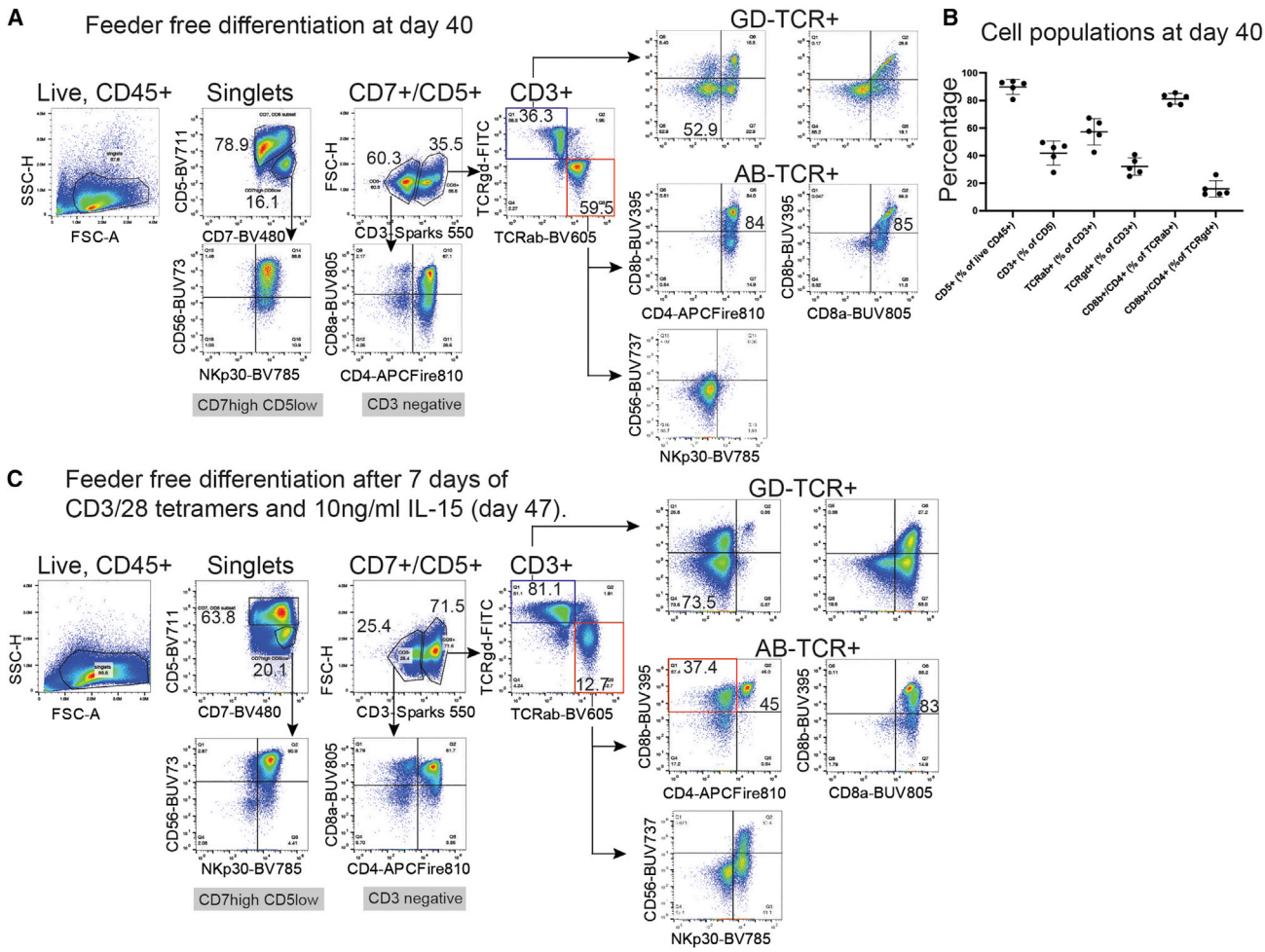

Figure 7. Feeder-free conditions support the emergence of alpha-beta T cells

(A) Feeder-free T cell differentiation analyzed using flow cytometry at day 40 with a broad panel of T cell markers.

(B) Using the same gating strategy as shown in (A), five separate differentiations (3 with 1N1, 2 with 3N1) were scored for the percentage of cells in each significant gate ($CD5^+$, $CD3^+$, $TCRab^+$, $TCRgd^+$, and CD8b/CD4 double-positive). A high degree of reproducibility across differentiations is demonstrated.

(C) The same flow cytometry panel is shown after one week of stimulation with CD3/CD28 tetramers and 10 ng/mL IL-15, demonstrating maturation of both TCRab (red square) and TCRgd populations (1N1 line).

$TCRab^+CD56^-$ which also expressed CD4, CD8a, and CD8b. In contrast, 30% of the $CD3^+$ cells were $TCRgd^+$ which were mostly negative for $CD4^-/CD8^-$ cells (Figure 7A). Remarkably, the percentages of these different populations were highly consistent across 5 independent differentiations (Figure 7B), providing strong evidence for the robustness of our platform. Upon stimulation with CD3/CD28 tetramers in the presence of IL-15 for one week, the cells show signs of maturation as evidenced by significant increase in $CD3^+$ cells (up to 72%), and the emergence of a $CD4^-$CD8ab single-positive $TCRab^+$ T cells (Figure 7C).

To further verify these $TCRab^+$ cells were progressing through a normal developmental program, we pursued RNA-based TCR sequencing on day 54 iPSC-derived T cells compared with PBMC controls (Figures S5A and S5B). Although the TCR diversity of iPSC-derived T cells was lower than control T cells, it still demonstrated broad use of V and J gene segments, with higher diversity for J segments. These results lend additional support to the emergence of polyclonal alpha-beta T cells from our differentiation cultures.

DISCUSSION

Using an inducible system to activate Notch signaling, we identified a critical 72 h window during early mesodermal differentiation when activation of the Notch pathway

induces a profound increase in T-capable multi-potent hematopoietic progenitors. The robustness of this finding was validated across four separate iPSC lines, strongly supporting the intrinsic role of Notch independent of genetic confounders. Importantly, our TetOn system allows Notch stimulation prior to the endogenous expression of the Notch1 receptor or Notch ligands. This is in contrast to other reports of Notch activation during hematopoietic differentiation that depend on the use of feeder cells expressing Notch ligands or DLL4-fc fusion proteins (Schmitt et al., 2004; Uenishi et al., 2018). Our results suggest that early Notch activation immediately after exit from pluripotency is a missing signal in hematopoietic mesodermal differentiation that allows more robust and consistent access to T/NK-capable progenitors. Our mesodermal differentiation is dependent on simultaneous activation of the Notch and WNT pathways. The importance of these pathways in early HSC development has been demonstrated in zebrafish, in which non-canonical WNT activation by Wnt16 was required for somitic expression of Notch ligands that delivered required Notch signals to migrating lateral plate mesodermal cells to allow HSC development (Clements et al., 2011). It is possible that the induced Notch expression in our system compensates for the loss of cross-talk between these cell populations in our differentiations. Notably, we tested whether inducing NICD1 with doxycycline could replace the signals provided by the OP9:hDLL4 or the Fc_DLL4 coated plates but did not observe the emergence of lymphoid progenitors by day 19 (data not shown). This suggests that ligand-receptor interactions provide a broader signal that is lost by NICD1 induction alone.

Our iPSC-derived T cells are not blocked at the $CD4^+$/$CD8^+$ double-positive stage, but progress even without stimulation to a $CD3^+$/$CD8^+$ T cell, with a small population of putative CD4 SP cells. The T cell identity of our cells was supported on flow cytometry, gene expression, stimulation data, and finally single-cell RNA sequencing. The strong bias toward CD8 SP cells was observed even though our feeder cells were engineered to express human MHC class II (DPα, DPβ, and CD74 from an EF1α-driven polycistronic lentiviral construct). Although the bias of iPSC-derived T cells is a general outcome in most if not all other reported T cell differentiation protocols (Awong et al., 2011; Iriguchi et al., 2021; Minagawa et al., 2018; Montel-Hagen et al., 2019), it has been unclear what cells participate in antigen presentation for positive selection. Although not conclusive evidence, the strong CD8 bias present in our engineered OP9-hDLL4:hMHCII co-culture suggests that the OP9 feeder cells are not participating as APCs in a meaningful way. It is also possible, however, that exposing the progenitors to the hMHC-II expressing OP9 cells must occur at a specific time during T cell differentiation to help the selection of CD4 SP cells, a possibility that warrants further investigation.

Notably, our protocol proceeds through differentiation all the way to CD8 SP T cells in the absence of any specific engineered T cell receptor, in contrast to most other reports (Awong et al., 2011; Iriguchi et al., 2021; Minagawa et al., 2018). Under feeder-free conditions, selection appears to be controlled by CD3/CD28 tetramer stimulation which was required to drive maturation into CD8SP cells. This was not the case in the OP9 system, in which emergence of CD8SP cells occurred in the absence of exogenous stimulation.

In other developmental contexts, Notch signaling has been shown to have density or dose-dependent effects. In the chick inner ear, hair producing cells and non-hair cells appear to be determined by the contact area between Notch signal sending and receiving cells (Shaya et al., 2017). In another study, Notch signaling regulated a cell-density dependent apoptosis pathway in NIH 3T3 cells (Matsuno et al., 2018). Even within the lymphoid lineage, low-level Notch signaling improved B cell differentiation, while high-level activation pushed cells toward the T cell lineage (Dallas et al., 2005). These studies suggest that Notch signal intensity is regulated by cell density, as would be predicted by the strict requirement for cell-cell interaction for productive Notch signaling (Bray, 2016). In our studies, the density of hematopoietic progenitors introduced into the co-culture system had a major impact on the T versus NK lineage choice. This could be due to the increased access of developing T cells to Notch ligands when plated at low density, suggesting that NK cell differentiation proceeds vigorously under slightly lower intensity Notch activation than T cells. In support of this idea, NK differentiation proceeded even in the presence of a low concentration of gamma-secretase inhibitor (data not shown).

Our single-cell RNA sequencing time course supports a marked enrichment of multi-potent hematopoietic progenitors in the dox-treated group that then progress toward the T cell lineage. A recent comprehensive paper described single-cell RNA sequencing of human embryonic and fetal early thymic progenitors (ETP) (Zeng et al., 2019). An early ETP was defined by a gene signature of *CD34*, *SPINK2*, *TRDC*, *RUNX3*, and *IGLL1*. In our dataset, day 12 progenitors are positive for *CD34* and *SPINK2*, but it takes 4 days of co-culture until day 16 before they begin to express *IGLL1* and *TRGC2*. This indicates our day 12 cells may represent an earlier stage progenitor. A later ETP (ETP2) was defined by a gene expression signature of *PTCRA*, *RAG1/2*, *CD3E/G*, *CD8B*, and lineage-defining transcription factors *BCL11B* and *TCF7*. In our dataset, all these genes turn on in the day 16 to day 20 transition and their expression levels are high by day 42 (both in single-cell data as well

as qRT-PCR). These similarities provide strong evidence supporting a similar developmental process in our cells compared with *in vivo* data. By day 42, our cells show a clear separation of T and NK cell clusters. Within the NK cell cluster, many genes consistent with both NK cells and innate-like lymphocytes (ILCs) are expressed, suggesting that this group may represent a mixture of NK and ILC fates that have not yet diverged at the transcriptional level. This is also true within the T cell cluster, where broad expression of *TRBC2* and *TRGC2* suggest both gamma-delta and alpha-beta T cells are present but not yet transcriptionally distinct. These results are consistent with early sampling at day 42, as flow cytometry data does not show a clear $CD8^+CD3^+$ SP population until day 63.

In summary, we describe a robust platform for the derivation of T/NK cells from iPSCs. In particular, Notch activation during early mesodermal differentiation has a marked impact on the production of multi-potent hematopoietic progenitors. These progenitors are not earmarked for the lymphoid lineage but have clear myeloid and erythroid potential. They follow an elegant developmental pathway toward the T/NK lineage with robust emergence of the T cell identity beginning by day 20 with clear similarity to primary human T cell development. The efficient derivation of an iPSC-derived T/NK lineage cell has important therapeutic implications for CAR-T therapy. Using gene-editing techniques prior to differentiation to introduce desired CARs, safety switches, and reduce immunogenicity would yield a potentially safer therapy with broader "off the shelf" capacity. In addition, our system could yield biological insights on T cell development that are otherwise difficult to probe, including specific signaling events leading to CD4 SP T cell development.

EXPERIMENTAL PROCEDURES

Tissue culture conditions and cell lines

OP9 cells (Mouse, ATCC CRL-2749) were maintained in alpha MEM supplemented with 20% FBS, 1× GlutaMAX, 1-thioglycerol, and Primocin at 37°C, 5% CO_2 in standard incubators (for reagents, resources, and primers, see Table S5). Cells were passaged using 0.05% trypsin every 3–4 days. 293 T cells were maintained as above but using DMEM with 10%FBS, 1× GlutaMAX, and Primocin. Human iPSC lines were maintained in tissue-culture treated 6-well plates coated with hESC-qualified Matrigel in mTeSR media with added Primocin. Media was changed every day except for weekends, when one day was skipped and the cells fed twice the normal volume. Cells were split weekly using ReLeSR following the manufacturer's protocol. Cells were grown at 37°C, 5% CO_2 in standard incubators. Specific iPSC lines used in this study were bBU1c2 (XY, EF1a-hSTEMCCA4 loxp lentiviral infection, Cre-excised), BU2-15-Cr10 (XY, EF1a-hSTEMCCA4 loxp lentiviral infection, Cre-excised), BU3-10-Cr1 (XY, EF1a-hSTEMCCA4 loxp lentiviral infection, Cre-excised), BU8.3 (XX, Sendai virus-based infection), and BU6 (XY, EF1a-hSTEMCCA4 loxp lentiviral infection). For bBU1c2, BU2, BU3, and BU8, a TetOn:NICD1 version was made and referred to as 1N1, 2N1, 3N1, and 8N1 respectively (see generation of iPSC TetOn:NICD1 lines). Anonymized pediatric human thymus samples were obtained under institutional review board (IRB) exemption through Boston Children's Hospital Cardiac Surgery Service.

Generation of iPSC TetOn:NICD1 lines

Control of Notch activation in iPSCs was pursued by creating a TetOn:NICD1 construct inserted into the AAVS1 safe harbor locus using zinc finger nucleases. See supplemental experimental procedures.

Differentiation into hematopoietic progenitors and T/NK cells

For differentiation to hematopoietic progenitors, iPSCs were plated at low confluency (~30–50 × 10^3/well) on Matrigel (catalog #354234; Corning) coated 6-well plates in mTeSR. Two days later, differentiations were begun by removing the mTeSR completely, adding the differentiation media for day 0, and transferring to hypoxic incubator (5% O_2). All differentiations begin on day 0; for example, "days 0–2" refers to a 3 day (72 h) period.

Single-cell analysis

Cells were differentiated per the "iT protocol," above with and without doxycycline at days 0–2. Cells were taken for single-cell analysis at day 12 (dox-treated and untreated), days 13, 16, 20, and 42 (after day 12, only dox-treated samples), and freshly isolated human thymocytes. We ran biological duplicates (two independent differentiations) of all samples except the human thymus. Cells were sorted for live, $CD45^+$ cells as outlined above in Cell Isolation and single cell isolation and library preparation was done using the inDrops method at the Harvard Single Cell Core followed by library sequencing at the Boston University Medical Center Microarray and Sequencing core.

Quantification and statistical analysis

For quantitative real-time PCR, fold change was calculated using the delta-delta CT method with BACT as a housekeeping gene. Results were then compared with the control state (usually iPSCs) using a two-tailed t test on $\log_{10}$ transformed expression values. Significance was assigned at a p value less than 0.05. For differentiations, N was variable and is noted in the figure legends.

Data and code availability

Single-cell RNAseq data were deposited at the Gene Expression Omnibus (GEO) (accession number GSE156111). Raw data and unique cell lines are available by request from the corresponding author or the Boston University Medical Campus Center for Regenerative Medicine iPSC Core Facility.

SUPPLEMENTAL INFORMATION

Supplemental information can be found online at https://doi.org/10.1016/j.stemcr.2022.10.007.

AUTHOR CONTRIBUTIONS

D.H. and G. Mostoslavsky. designed the project, developed experiments, analyzed data, and wrote the manuscript. D.H. performed the experiments. S.P., M.H., A. McCracken, A. Mithal, M.W.Y., and G. Murphy designed and performed additional experiments. C.V.-M., J.L., and F.W. performed the bioinformatics analysis.

ACKNOWLEDGMENTS

We thank Dr. Tony Godfrey and Dr. Donald Hess and the Department of Surgery at Boston University Medical Center, Anna Belkina and Brian Tilton at the Boston University School of Medicine (BUSM) flow cytometry core, the Harvard Single-Cell Core, the Boston University Microarray and Sequencing Core, Dr. Meena Nathan and Angelika Muter at Boston Children's Hospital, and also Darrell Kotton and Jonathan Duke-Cohen for feedback and fruitful discussions. D.H. was supported in part by National Institute of General Medical Sciences (NIGMS) grant 5F32HL149605-02. G. Mostoslavsky is supported by National Heart, Lung, and Blood Institute (NHLBI) grant N01-75N92020C00005.

CONFLICT OF INTERESTS

Boston Medical Center has filed a patent application on the findings of this manuscript. G. Mostoslavsky is a scientific founder of and holds equity in Clade Therapeutics.

Received: November 16, 2021
Revised: October 6, 2022
Accepted: October 7, 2022
Published: December 13, 2022

REFERENCES

Awong, G., Herer, E., La Motte-Mohs, R.N., and Zúñiga-Pflücker, J.C. (2011). Human CD8 T cells generated in vitro from hematopoietic stem cells are functionally mature. BMC Immunol. *12*, 22.

Bijl, J., Thompson, A., Ramirez-Solis, R., Krosl, J., Grier, D.G., Lawrence, H.J., and Sauvageau, G. (2006). Analysis of HSC activity and compensatory Hox gene expression profile in Hoxb cluster mutant fetal liver cells. Blood *108*, 116–122. https://doi.org/10.1182/blood-2005-06-2245.

Böiers, C., Carrelha, J., Lutteropp, M., Luc, S., Green, J.C.A., Azzoni, E., Woll, P.S., Mead, A.J., Hultquist, A., Swiers, G., et al. (2013). Lymphomyeloid contribution of an immune-restricted progenitor emerging prior to definitive hematopoietic stem cells. Cell Stem Cell *13*, 535–548. https://doi.org/10.1016/j.stem.2013.08.012.

Bray, S.J. (2016). Notch signalling in context. Nat. Rev. Mol. Cell Biol. *17*, 722–735. https://doi.org/10.1038/nrm.2016.94.

Campanelli, D., Detmers, P.A., Nathan, C.F., and Gabay, J.E. (1990). Azurocidin and a homologous serine protease from neutrophils. Differential antimicrobial and proteolytic properties. J. Clin. Invest. *85*, 904–915. https://doi.org/10.1172/JCI114518.

Challen, G.A., Sun, D., Mayle, A., Jeong, M., Luo, M., Rodriguez, B., Mallaney, C., Celik, H., Yang, L., Xia, Z., et al. (2014). Dnmt3a and Dnmt3b have overlapping and distinct functions in hematopoietic stem cells. Cell Stem Cell *15*, 350–364. https://doi.org/10.1016/j.stem.2014.06.018.

Chen, E.Y., Tan, C.M., Kou, Y., Duan, Q., Wang, Z., Meirelles, G.V., Clark, N.R., and Ma'ayan, A. (2013). Enrichr: interactive and collaborative HTML5 gene list enrichment analysis tool. BMC Bioinf. *14*, 128. https://doi.org/10.1186/1471-2105-14-128.

Clements, W.K., Kim, A.D., Ong, K.G., Moore, J.C., Lawson, N.D., and Traver, D. (2011). A somitic Wnt16/Notch pathway specifies haematopoietic stem cells. Nature *474*, 220–224. https://doi.org/10.1038/nature10107.

Dallas, M.H., Varnum-Finney, B., Delaney, C., Kato, K., and Bernstein, I.D. (2005). Density of the Notch ligand Delta1 determines generation of B and T cell precursors from hematopoietic stem cells. J. Exp. Med. *201*, 1361–1366. https://doi.org/10.1084/jem.20042450.

Ditadi, A., and Sturgeon, C.M. (2016). Directed differentiation of definitive hemogenic endothelium and hematopoietic progenitors from human pluripotent stem cells. Methods *101*, 65–72. https://doi.org/10.1016/j.ymeth.2015.10.001.

Ditadi, A., Sturgeon, C.M., Tober, J., Awong, G., Kennedy, M., Yzaguirre, A.D., Azzola, L., Ng, E.S., Stanley, E.G., French, D.L., et al. (2015). Human definitive haemogenic endothelium and arterial vascular endothelium represent distinct lineages. Nat. Cell Biol. *17*, 580–591. https://doi.org/10.1038/ncb3161.

Fish, J.E., and Wythe, J.D. (2015). The molecular regulation of arteriovenous specification and maintenance. Dev. Dynam. *244*, 391–409. https://doi.org/10.1002/dvdy.24252.

Gordon, W.R., Zimmerman, B., He, L., Miles, L.J., Huang, J., Tiyanont, K., McArthur, D.G., Aster, J.C., Perrimon, N., Loparo, J.J., and Blacklow, S.C. (2015). Mechanical allostery: evidence for a force requirement in the proteolytic activation of notch. Dev. Cell *33*, 729–736. https://doi.org/10.1016/j.devcel.2015.05.004.

Hadland, B.K., Huppert, S.S., Kanungo, J., Xue, Y., Jiang, R., Gridley, T., Conlon, R.A., Cheng, A.M., Kopan, R., and Longmore, G.D. (2004). A requirement for Notch1 distinguishes 2 phases of definitive hematopoiesis during development. Blood *104*, 3097–3105. https://doi.org/10.1182/blood-2004-03-1224.

Iriguchi, S., Yasui, Y., Kawai, Y., Arima, S., Kunitomo, M., Sato, T., Ueda, T., Minagawa, A., Mishima, Y., Yanagawa, N., et al. (2021). A clinically applicable and scalable method to regenerate T-cells from iPSCs for off-the-shelf T-cell immunotherapy. Nat. Commun. *12*, 430. https://doi.org/10.1038/s41467-020-20658-3.

Joshi, I., Minter, L.M., Telfer, J., Demarest, R.M., Capobianco, A.J., Aster, J.C., Sicinski, P., Fauq, A., Golde, T.E., and Osborne, B.A. (2009). Notch signaling mediates G1/S cell-cycle progression in T cells via cyclin D3 and its dependent kinases. Blood *113*, 1689–1698. https://doi.org/10.1182/blood-2008-03-147967.

Kitaguchi, T., Kawakami, K., and Kawahara, A. (2009). Transcriptional regulation of a myeloid-lineage specific gene lysozyme C during zebrafish myelopoiesis. Mech. Dev. *126*, 314–323. https://doi.org/10.1016/j.mod.2009.02.007.

Kuleshov, M.V., Jones, M.R., Rouillard, A.D., Fernandez, N.F., Duan, Q., Wang, Z., Koplev, S., Jenkins, S.L., Jagodnik, K.M., Lachmann, A., et al. (2016). Enrichr: a comprehensive gene set enrichment analysis web server 2016 update. Nucleic Acids Res. *44*, W90–W97. https://doi.org/10.1093/nar/gkw377.

Kumano, K., Chiba, S., Kunisato, A., Sata, M., Saito, T., Nakagami-Yamaguchi, E., Yamaguchi, T., Masuda, S., Shimizu, K., Takahashi, T., et al. (2003). Notch1 but not Notch2 is essential for generating hematopoietic stem cells from endothelial cells. Immunity *18*, 699–711.

Lawrence, H.J., Christensen, J., Fong, S., Hu, Y.L., Weissman, I., Sauvageau, G., Humphries, R.K., and Largman, C. (2005). Loss of expression of the Hoxa-9 homeobox gene impairs the proliferation and repopulating ability of hematopoietic stem cells. Blood *106*, 3988–3994. https://doi.org/10.1182/blood-2005-05-2003.

Leung, A., Zulick, E., Skvir, N., Vanuytsel, K., Morrison, T.A., Naing, Z.H., Wang, Z., Dai, Y., Chui, D.H.K., Steinberg, M.H., et al. (2018). Notch and aryl hydrocarbon receptor signaling impact definitive hematopoiesis from human pluripotent stem cells. Stem Cell. *36*, 1004–1019. https://doi.org/10.1002/stem.2822.

Matsuno, Y., Kiwamoto, T., Morishima, Y., Ishii, Y., Hizawa, N., and Hogaboam, C.M. (2018). Notch signaling regulates cell density-dependent apoptosis of NIH 3T3 through an IL-6/STAT3 dependent mechanism. Eur. J. Cell Biol. *97*, 512–522. https://doi.org/10.1016/j.ejcb.2018.09.001.

Minagawa, A., Yoshikawa, T., Yasukawa, M., Hotta, A., Kunitomo, M., Iriguchi, S., Takiguchi, M., Kassai, Y., Imai, E., Yasui, Y., et al. (2018). Enhancing T cell receptor stability in rejuvenated iPSC-derived T cells improves their use in cancer immunotherapy. Cell Stem Cell *23*, 850–858.e4. https://doi.org/10.1016/j.stem.2018.10.005.

Miyazaki, T., Kato, I., Takeshita, S., Karasuyama, H., and Kudo, A. (1999). Lambda5 is required for rearrangement of the Ig kappa light chain gene in pro-B cell lines. Int. Immunol. *11*, 1195–1202. https://doi.org/10.1093/intimm/11.8.1195.

Montel-Hagen, A., Seet, C.S., Li, S., Chick, B., Zhu, Y., Chang, P., Tsai, S., Sun, V., Lopez, S., Chen, H.C., et al. (2019). Organoid-induced differentiation of conventional T cells from human pluripotent stem cells. Cell Stem Cell *24*, 376–389.e8. https://doi.org/10.1016/j.stem.2018.12.011.

Niemann, C.U., Abrink, M., Pejler, G., Fischer, R.L., Christensen, E.I., Knight, S.D., and Borregaard, N. (2007). Neutrophil elastase depends on serglycin proteoglycan for localization in granules. Blood *109*, 4478–4486. https://doi.org/10.1182/blood-2006-02-001719.

Noseda, M., Chang, L., McLean, G., Grim, J.E., Clurman, B.E., Smith, L.L., and Karsan, A. (2004). Notch activation induces endothelial cell cycle arrest and participates in contact inhibition: role of p21Cip1 repression. Mol. Cell Biol. *24*, 8813–8822. https://doi.org/10.1128/MCB.24.20.8813-8822.2004.

Paul, F., Arkin, Y., Giladi, A., Jaitin, D.A., Kenigsberg, E., Keren-Shaul, H., Winter, D., Lara-Astiaso, D., Gury, M., Weiner, A., et al. (2015). Transcriptional heterogeneity and lineage commitment in myeloid progenitors. Cell *163*, 1663–1677. https://doi.org/10.1016/j.cell.2015.11.013.

Popescu, D.M., Botting, R.A., Stephenson, E., Green, K., Webb, S., Jardine, L., Calderbank, E.F., Polanski, K., Goh, I., Efremova, M., et al. (2019). Decoding human fetal liver haematopoiesis. Nature *574*, 365–371. https://doi.org/10.1038/s41586-019-1652-y.

Roth, J., Vogl, T., Sorg, C., and Sunderkötter, C. (2003). Phagocyte-specific S100 proteins: a novel group of proinflammatory molecules. Trends Immunol. *24*, 155–158. https://doi.org/10.1016/s1471-4906(03)00062-0.

Schmitt, T.M., de Pooter, R.F., Gronski, M.A., Cho, S.K., Ohashi, P.S., and Zúñiga-Pflücker, J.C. (2004). Induction of T cell development and establishment of T cell competence from embryonic stem cells differentiated in vitro. Nat. Immunol. *5*, 410–417. https://doi.org/10.1038/ni1055.

Shah, D.K., and Zúñiga-Pflücker, J.C. (2014). An overview of the intrathymic intricacies of T cell development. J. Immunol. *192*, 4017–4023. https://doi.org/10.4049/jimmunol.1302259.

Shaya, O., Binshtok, U., Hersch, M., Rivkin, D., Weinreb, S., Amir-Zilberstein, L., Khamaisi, B., Oppenheim, O., Desai, R.A., Goodyear, R.J., et al. (2017). Cell-cell contact area affects notch signaling and notch-dependent patterning. Dev. Cell *40*, 505–511.e6. https://doi.org/10.1016/j.devcel.2017.02.009.

Singh, S.K., Singh, S., Gadomski, S., Sun, L., Pfannenstein, A., Magidson, V., Chen, X., Kozlov, S., Tessarollo, L., Klarmann, K.D., and Keller, J.R. (2018). Id1 ablation protects hematopoietic stem cells from stress-induced exhaustion and aging. Cell Stem Cell *23*, 252–265.e8. https://doi.org/10.1016/j.stem.2018.06.001.

Takata, K., Kozaki, T., Lee, C.Z.W., Thion, M.S., Otsuka, M., Lim, S., Utami, K.H., Fidan, K., Park, D.S., Malleret, B., et al. (2017). Induced-pluripotent-stem-cell-derived primitive macrophages provide a platform for modeling tissue-resident macrophage differentiation and function. Immunity *47*, 183–198.e6. https://doi.org/10.1016/j.immuni.2017.06.017.

Terstappen, L.W., Huang, S., and Picker, L.J. (1992). Flow cytometric assessment of human T-cell differentiation in thymus and bone marrow. Blood *79*, 666–677.

Themeli, M., Kloss, C.C., Ciriello, G., Fedorov, V.D., Perna, F., Gonen, M., and Sadelain, M. (2013). Generation of tumor-targeted human T lymphocytes from induced pluripotent stem cells for cancer therapy. Nat. Biotechnol. *31*, 928–933. https://doi.org/10.1038/nbt.2678.

Tian, Y., Xu, J., Feng, S., He, S., Zhao, S., Zhu, L., Jin, W., Dai, Y., Luo, L., Qu, J.Y., and Wen, Z. (2017). The first wave of T lymphopoiesis in zebrafish arises from aorta endothelium independent of hematopoietic stem cells. J. Exp. Med. *214*, 3347–3360. https://doi.org/10.1084/jem.20170488.

Tyser, R.C.V., Mahammadov, E., Nakanoh, S., Vallier, L., Scialdone, A., and Srinivas, S. (2021). Single-cell transcriptomic characterization of a gastrulating human embryo. Nature *600*, 285–289. https://doi.org/10.1038/s41586-021-04158-y.

Uenishi, G.I., Jung, H.S., Kumar, A., Park, M.A., Hadland, B.K., McLeod, E., Raymond, M., Moskvin, O., Zimmerman, C.E., Theisen, D.J., et al. (2018). NOTCH signaling specifies arterial-type definitive hemogenic endothelium from human pluripotent stem cells. Nat. Commun. *9*, 1828. https://doi.org/10.1038/s41467-018-04134-7.

Yoshimoto, M., Porayette, P., Glosson, N.L., Conway, S.J., Carlesso, N., Cardoso, A.A., Kaplan, M.H., and Yoder, M.C. (2012). Autonomous murine T-cell progenitor production in the extra-embryonic yolk sac before HSC emergence. Blood *119*, 5706–5714. https://doi.org/10.1182/blood-2011-12-397489.

Zeng, Y., Liu, C., Gong, Y., Bai, Z., Hou, S., He, J., Bian, Z., Li, Z., Ni, Y., Yan, J., et al. (2019). Single-cell RNA sequencing resolves spatiotemporal development of pre-thymic lymphoid progenitors and thymus organogenesis in human embryos. Immunity *51*, 930–948.e6. https://doi.org/10.1016/j.immuni.2019.09.008.